PROLONGED BOULDER EXHUMATION AT THE RIMS OF KILOMETER-SCALE CRATERS ON THE LUNAR MARIA. C. A. Nypaver[1], B. J. Thomson[1], E. G. Rivera-Valentín[2], C. I. Fassett[3], C. D. Neish[4], G. W. Patterson[5], A. K. Virkki[6], P. A. Taylor[2]. [1]The University of Tennessee, Knoxville, 1621 Cumberland Ave, 602 Strong Hall, Knoxville, TN 37996 (cnypaver@vols.utk.edu). [2]Lunar and Planetary Institute, USRA, Houston, TX 77058. [3]NASA MSFC, Huntsville, AL 35805. [4]Department of Earth Sciences, The University of Western Ontario, London, Ontario, N6A 5B7, [5]Johns Hopkins Applied Physics Laboratory, Laurel, MD 2027. [6] Arecibo Observatory, University of Central Florida, Arecibo, PR.

Introduction and Background: Boulders associated with lunar impact ejecta deposits break down over time due to meteoroid bombardment and thermal fatigue [e.g., 1, 2]. This breakdown process has been studied using high-resolution, optical images from the Lunar Reconnaissance Orbiter Camera (LROC) [e.g., 3]. Those studies agree that even the largest boulders on the lunar surface should be destroyed within ~300 Myr. Furthermore, prior studies which model the rock breakdown process using remote sensing data, showed that boulders associated with lunar ejecta deposits break down at a measurable rate that may serve as an independent means of inferring crater age dates [e.g., 4–8].

In the work presented here, we observe meter-scale boulders in LROC NAC images at the rims of older (~2.0–3.5 Ga) km-scale impact craters on the lunar maria. From these observations, we hypothesize that a population of boulders can be found at crater rims for a long period of time. We test this hypothesis by comparing the ejecta and rim rock populations of 6,222 km-scale impact craters on the lunar maria using S-band monostatic radar data from the LRO Mini-RF instrument [9] and rock abundance data derived from LRO Diviner thermal measurements [11]. Our results indicate that rocks at impact crater rims are exhumed for the entirety of a crater's lifetime by the downslope creep of the overlying regolith.

Methods: The derived radar products used to measure rock populations in this work are total power, same-sense circular polarization (SC) and circular polarization ratio (CPR) data from the Mini-RF instrument [9]. The SC data used here represents diffuse scattering from the lunar surface and subsurface, while the ratio of the SC and OC (opposite-sense circular polarization) data comprises the CPR dataset. The SC and CPR data are sensitive to lunar rocks on the order of the S-band wavelength (~12.6 cm) at the lunar surface and down to a depth that is some 10× that wavelength [e.g., 10]. The second remote sensing dataset used here are Rock Abundance (RA) data derived from thermal measurements recorded by the LRO Diviner Thermal Radiometer instrument [11]. The RA data utilize the anisothermality of rocks and regolith at the lunar surface to infer the lunar surface rock concentration and regolith temperature given an assumed rock temperature. These RA data are sensitive to meter-scale rocks at the lunar surface only (i.e., within a diurnal skin depth).

The individual craters in our sample set possess model ages that were derived from their topographic degradation states in a prior study [12]. A shapefile depicting the center coordinates of all craters was imported into ArcMap 10.6 and polygons were drawn over the crater rims and ejecta. The mean SC total power, CPR, and RA values were then collected for each polygon using the ArcMap zonal statistics tool and binned for comparison with corresponding age values.

Results: A comparison of SC, CPR, and RA as a function of age for the crater rim and ejecta indicates that values associated with crater rims and ejecta decrease with time (**Fig. 1**). Moreover, the measured values associated with crater rims remain elevated above measured ejecta values for all crater bins in some datasets. This difference between rim and ejecta values is more substantial earlier in the craters lifetime and diminishes over time. The crater rim values reach a steady-state increase over the ejecta at ~2.0 Ga in all three datasets. The separation between crater rims and ejecta at the beginning of a crater's lifetime measures as a difference of ~0.06 in RA, ~0.1 in CPR, and ~0.06 in SC. As a proof of concept, we also test these relationships using S-band CPR data collected by the Mini-RF instrument in bistatic configuration [13], i.e., using Arecibo as a transmitter and Mini-RF as a receiver for the scattered echoes from the lunar surface. Although the sample size of craters in bistatic data is small (5 craters), the trend of increased surface and subsurface rim rock populations also holds true in these data.

Discussion: The observed differences in CPR, SC, and RA data for impact crater rims and ejecta suggests that an increased rock population exists at crater rims compared to ejecta. While the difference in rock population is greatest early in the crater's lifetime, the results indicate that an increased rock population persists at crater rims to a lesser degree for the lifetime of km-scale craters on the lunar maria. The crater rim-ejecta difference is most pronounced in the RA data, which are sensitive to surface rocks only. As the initial population of surface rocks breaks down, the difference in crater rim and ejecta RA decreases by ~60%. The sensitivity of the radar data to surface and subsurface rocks leads to a less dramatic evolution of CPR and SC

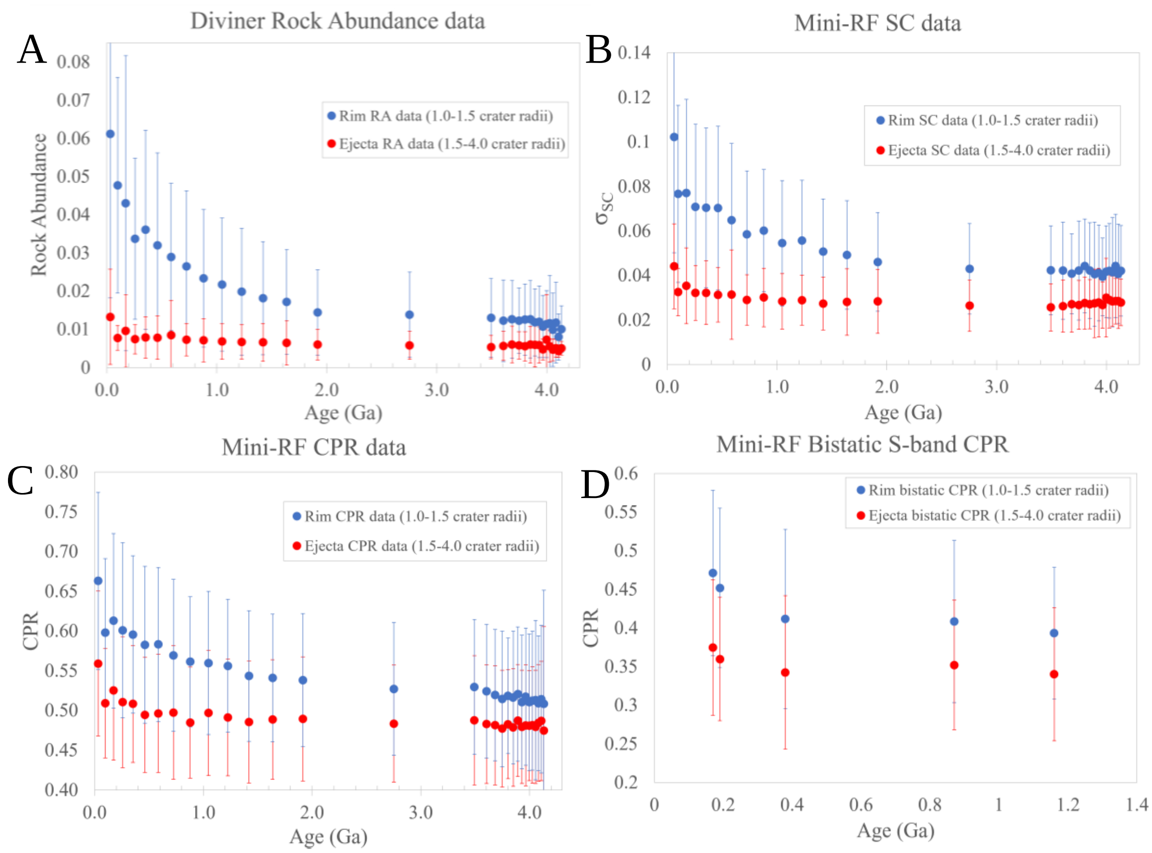

Figure 1: Binned RA (**a**), CPR (**b**), SC total power (**c**), and Mini-RF bistatic CPR (**d**) data for crater rims and ejecta plotted as a function of increasing crater age. Data averages for crater rims (blue points) remain elevated above ejecta (red points) in all datasets and bins. The consistent trend among the bistatic CPR indicates that our primary results may be replicable in new data collected by the ongoing Mini-RF bistatic campaign. Craters are binned by degradation state and then plotted based on the corresponding age. Each bin contains ~50–200 craters.

separation between crater rims and ejecta. While surface rocks in the ejecta deposit break down relatively quickly, we infer that subsurface rocks remain uneroded and lead to a consistent difference in crater rim and ejecta radar data through time.

The proposition that surface rock populations observed at crater rims have remained in place and uneroded for >2.0 Ga is unlikely and contradictory to an abundance of robust prior work [e.g., 3]. Rather, we attribute the prolonged crater rim rock populations to a boulder exhumation process acting at the topographically high impact crater rims [see also 6]. Over time, regolith at crater rims migrates downslope into the crater interior and towards the edge of the proximal ejecta. This downslope motion of regolith exhumes the underlying rocks over time to retain an enhanced rock population at crater rims.

Conclusions: Our results suggest that rocks are continuously being exhumed at crater rims due to the downslope motion of the overlying regolith. The net effect of this exhumation process is an elevated rock population at km-scale crater rims for prolonged periods of time. Therefore, the rocks at km-scale impact crater rims are unlikely to have undergone distal transport, making them ideal candidates for future lunar sampling initiatives. An alternate hypothesis for the heightened crater rim rock populations is the prolonged breakdown of impact melt at crater rims [e.g., 14].

References: [1] Soderblom L. A. (1970) *JGR*, *75*, 2655-2661. [2] Molaro J. L. et al. (2017) *Icarus*, *294*, 247–261. [3] Basilevsky A. T. et al. (2013) *Planetary and Space Sci.*, *89*, 118–126. [4] Ghent R. R. et al. (2011) *Geology*, *42*(12), 1059–1062. [5] Bell S. W. et al. (2012) *JGR*, *117*, E12. [6] Fassett C. I. et al. (2018) *JGR*, *123*(12), 3133–3143. [7] Ghent R. R. et al. (2016) *Icarus*, *273*, 182-195. [8] Mazrouei S. et al. (2019) *Science*, *363*, 253–257. [9] Raney R. K. et al (2011) *Proc. IEEE*, *99*, 808–823. [10] Campbell B. A. (2010), *Icarus*, *208*, 565–573. [11] Bandfield J. L. et al. (2011) *JGR*, *116*, E12. [12] Fassett C. I. and Thomson B. J. (2014) *JGR*, *119*, 2255–2271. [13] Patterson G. W. et al. (2017) *Icarus*, *283*, 2–19. [14] Stopar J. D. et al. (2014) *Icarus*, *243*, 337–357.